Smart Structures Systems, *Vol. 19, No. 4 (2017) 371-382*
DOI: https://doi.org/10.12989/sss.2017.19.4.371

Monitoring degradation in concrete filled steel tubular sections using guided waves

Kumari Beena[*1], Sharma Shruti[1], Sharma Sandeep[2] and Kwatra Naveen[1]

[1]*Department of Civil Engineering, Thapar University, Patiala 147-001, India*
[2]*Department of Mechanical Engineering, Thapar University, Patiala 147-001, India*

(Received October 8, 2015, Revised December 10, 2016, Accepted December 22, 2016)

Abstract. Concrete filled steel tubes are extensively applied in engineering structures due to their resistance to high tensile and compressive load and convenience in construction. But one major flaw, their vulnerability to environmental attack, can severely reduce the strength and life of these structures. Degradation due to corrosion of steel confining the concrete is one of the major durability problems faced by civil engineers to maintain these structures. The problem accelerates as inner surface of steel tube is in contact with concrete which serves as electrolyte. If it remains unnoticed, it further accelerates and can be catastrophic. This paper discusses a non-destructive degradation monitoring technique for early detection corrosion in steel tubes in CFST members. Due to corrosion, damage in the form of debonding and pitting occurs in steel sections. Guided ultrasonic waves have been used as a feasible and attractive solution for the detection and monitoring of corrosion damages in CFST sections. Guided waves have been utilized to monitor the effect of notch and debond defects in concrete filled steel tubes simulating pitting and delamination of steel tubes from surrounding concrete caused by corrosion. Pulse transmission has been used to monitor the healthy and simulated damaged specimens. A methodology is developed and successfully applied for the monitoring of concrete filled steel tubular sections undergoing accelerated chloride corrosion. The ultrasonic signals efficiently narrate the state of steel tube undergoing corrosion.

Keywords: guided waves; corrosion; notching; delamination; concrete filled steel tubular sections

1. Introduction

Concrete filled tubular steel (CFST) structures have gained popularity in supporting heavy loads in high rise buildings, bridges and offshore structures (Gourley *et al.* 2003). Many researchers agree that CFST members utilise the advantages of both steel and concrete as steel members have the advantages of high tensile strength and ductility, while concrete members may be advantageous in compressive strength and stiffness. These members also have excellent hysteresis behaviour under cyclic loading, compared with hollow tubes (Hajjar 2000). They are comprised of a steel hollow section of circular or rectangular shape filled with plain or reinforced concrete. CFST structural members have a number of distinctive advantages over conventional steel reinforced concrete members. CFST members provide excellent seismic resistance in two orthogonal directions as well as good damping characteristics (Elchalakani *et al.* 2001). The use of CFST members in moment resisting frames eliminates the use of additional stiffening elements in panel zones and zones of high strain demand. CFST columns have been proven to be cost effective in building structures compared to conventional reinforced concrete columns (Webb and Beyton 1990).

Steel tube of CFST members act as a permanent and integral formwork and support several levels of construction prior to concrete being poured. It also provides external reinforcement and higher strength and stiffness compare with RC sections of the same materials properties. The main effect of concrete is that it delays the local buckling of the tube wall and the concrete itself. These composite members can be also used for resisting outside pressure in seismic regions because of excellent earthquake-resistant properties such as high strength, high ductility, and large energy absorption capacity (Kuranovas and Kvedaras 2007). The beneficial composite action of these CFST members requires force transfer between the steel tube and the core concrete. The quality of concrete pumping and pouring, the change of temperature, the shrinkage and creep of the mass concrete core are some of the causes of interfacial debonding defect between the steel and inner concrete core of CFST. Yang *et al.* (2015) presented an experimental study of CFST columns and plain concrete columns, subjected to sustained axial loads for creep which cause interfacial debonding. The interfacial debonding defect can weaken the confinement effect of steel tube on the concrete core resulting into the loss of load-carrying capacity and in the ductility of the CFST under earthquake and cyclic loadings. Unfortunately, such debonding damage and the voids cannot be visually identified. Actually, these are almost unavoidable in CFST structures but such damages are most unfavorable (Xue *et al.* 2012). Another

∗Corresponding author, Ph.D. Student
E-mail: beena_ansh@yahoo.co.in
[a]Ph.D.
E-mail: shruti.sharma@thapar.edu

ISSN: 1738-1584 (Print), 1738-1991 (Online)

major flaw of structures made of CFST sections is their vulnerability to environmental attack causing corrosion. It can severely reduce the strength and life of these structures. Corrosion of steel confining the concrete is one of the major durability problems to maintain aging CFST structures. The problem accelerates since inner surface of steel tube is in contact with concrete which serves as electrolyte for the initiation of corrosion. If the corrosion ingress starts, it further accelerates and can be catastrophic for the structures as it results in huge loss of life and property. The increased volume of the corrosion products induces stresses in the concrete that result in cracking and delamination of steel tube from the in filled concrete. As a result, it weakens the structure to a high degree. Also, corrosion due to chloride ingress results in occurrence of pits in the steel tube which reduce the cross-sectional area of tube drastically and can be catastrophic.

A wide range of techniques have been reported in the literature that may be suitably employed for the monitoring of corrosion of steel in reinforced concrete structures for assessing the cause and extent of the corrosion. But most of the techniques are electrochemical techniques which relate corrosion rate and extent through assessment on surrounding concrete medium. None of the techniques focus on corrosion monitoring through direct measurements on steel tube. The degradation due to corrosion accelerates and can be catastrophic unless early remedial action is taken. Therefore, it is necessary to develop a non-intrusive technique for early detection of damages in the form of cracks, debonds and corrosion in steel tubes in CFST members. In this work, it is proposed to use ultrasonic guided waves for monitoring these damages in CFST sections. Guided waves have been used owing to their ability to scan through longer spans with sensitivity better than conventional non-destructive testing techniques. In addition, different frequencies and modes can be utilized for evaluation of different types of damages in RC structures.

Guided waves have been exploited by researchers recently for monitoring various types of damages like notches and debond etc. But in most of these studies, corrosion has been simulated by delamination of reinforcing bars. Na *et al.* (2002, 2003) utilized both high (1 MHz) and low frequencies (150 kHz) to study the effect of varying bond levels at steel-concrete interface and debond location in RC beams on the received waveforms. It was concluded that debond resulted in increase in signal for both low and high frequencies. He *et al.* (2006) studied the effect of debond on signals in cylindrical specimens using frequencies between 1 MHz and 2 MHz and found the lower frequencies sensitive to the change in bond. Ervin *et al.* (2008, 2009) also used both low (<200 kHz) and high (2-9 MHz) guided longitudinal modes to ultrasonically monitor the accelerated corrosion experiments. Some modes were found sensitive to the effect of bond deterioration and mortar stiffness reduction while others related well to the change in cross-sectional area. Reis *et al.* (2005) estimated corrosion damage in steel reinforced mortar using fundamental flexural mode at frequencies below 250 kHz. Debond defects were simulated by wrapping a tape around the rebar. Waveform energy indicative of the attenuation was used to relate to corrosion damage and the loss of bond between steel and surrounding concrete has been detected and evaluated. The ultrasonic investigations of corroded RC beams have mainly remained limited to simulated specimens. Effect of corrosion has mainly been viewed as loss of interfacial bond. Thus, higher signal strength at the receiving end has been indicative of debond and corrosion as debond obstructs the leakage of wave signals into concrete. Sharma and Mukherjee (2010) utilized longitudinal guided waves to monitor notch and debond defects in steel bars in concrete simulating pitting and delamination phenomena caused by corrosion. Two ultrasonic techniques of pulse transmission and pulse echo were used to monitor the healthy and damaged specimens. The developed methodology was successfully applied for real time monitoring of RC beam specimens undergoing accelerated chloride corrosion. Guided waves were further used for monitoring difference in progression of rebar corrosion in concrete in varying chloride and oxide environments (Sharma and Mukherjee 2010). The effect of rates of corrosion in the two environments on the ultrasonic signals was reported. Surface and core-seeking guided wave modes were used to monitor beams undergoing accelerated impressed current corrosion in the presence of chloride corrosion and absence of chlorides (oxide corrosion). Effective combination of guided wave modes could relate to the differences in corrosion mechanisms and rates in the two environments (Sharma and Mukherjee 2013).

Na *et al.* (2002) suggested the use of guided waves for inspection of pipes filled with concrete exposed in water. A special coupling mechanism for transmitting the guided waves has been introduced for the experimental study to study the feasibility of guided waves for underwater inspection of concrete-filled steel pipes. Xu *et al.* (2013) proposed a novel active interfacial debonding detection method for rectangular CFST sections based on the wavelet packet energy / spectrum of measurement of patches. Li *et al.* (2016) used acoustic emission (AE) signals technique to monitor the development of damage in CFRP-confined circular concrete-filled steel tubular columns and developed a fuzzy c-means method to determine the relationship between the AE signal and failure mechanisms.

The research in the last two decades has shown the capability of ultrasonic guided waves for monitoring various kinds of damages in RC structures. The technique has been used to monitor debonding of steel from concrete in CFST sections. But a more elaborate and detailed investigation of various kinds of damages in CFST sections is still required to develop a complete damage monitoring methodology for the same. In this paper, ultrasonic guided waves have been used in pulse transmission (PT) for monitoring two type of defects i.e., notches and delamination simulating loss of area and debond due to corrosion in CFST sections. Specific guided wave modes were used for investigating varying extents of notches and simulated delamination defects. PT signatures could relate to the percentage notch and delamination very efficiently. The method is further applied to CFST sections undergoing accelerated corrosion. It can successfully relate to the state of steel tube undergoing chloride corrosion and can be applied to real time corrosion monitoring of CFST sections. The methodology developed in the study clearly suggests that non-contact ultrasonic guided wave approach can be used for degradation monitoring in CFST sections.

2. Guided waves in CFST sections

Guided waves are the waves which travel along the medium guided by the geometric boundaries which has a strong influence on the behavior of the wave (Achenbach 1984, Redwood 1960). In contrast to ultrasonic bulk waves that propagate at a constant velocity, the velocity of the guided waves varies considerably with the wave frequency and the geometry of the medium. Also at a given wave frequency, the guided waves can propagate in different wave modes (Rose 2003) The complex effect of the boundaries results in dispersion of the wave and generates different modes that have predictable frequency-dependent properties. The velocity-frequency relationships of guided waves can be displayed as dispersion curves (Pavlakovic and Cawley 2000). Ultrasonic Guided Wave inspection and structural health monitoring is being considered in such natural wave guide structures as plates, multi-layer structures, rods, rails, piping and tubing (Rose *et al.* 2004) A major advantage of guided waves is inspection over long distances with excellent sensitivity from a probe position.

In CFST section, desired Lamb waves can be excited in the steel tube just as in the steel plates. The ultrasonic wave is reflected from its boundaries, and the energy is contained within the steel tube as a guided Lamb wave. The complex effect of the steel tube boundaries surrounded by air on the one side and concrete on the other, results in dispersion of the wave and generates different modes. Various Lamb wave modes can be effectively generated by a pair of transducers arranged in a pitch catch orientation and having equal inclination with steel tube using water as coupling media. At a particular frequency, the different Lamb wave modes can be produced by varying the angle of the transmitting and receiving probes (Fig. 1), calculated by Snell's law as-

$$\theta=\sin^{-1}(VL/V_{ph}) \tag{1}$$

where,

V_{Ph}= Phase velocity of the desired Lamb Wave mode

V_L=Longitudinal velocity of the incident wave in the coupling media.

For generating specific ultrasonic guided wave mode, an acrylic tank of dimensions 350 mm×70 mm×70 mm was fixed on the top of CFST specimen to maneuver the probes and water was used as coupling media to carry the incident energy from the probe to the tube surface (Fig. 1(b)). The scanning of a particular length of CFST section was done in pitch catch orientation by the transmitter and receiver probes placed at same angle of inclination with vertical (θ) as shown in Fig. 1. Both the probes are kept at same inclination with vertical to make the receiver most sensitive to the wavelength of the input frequency.

The specific Lamb waves transmit through the length of the tube and should be sensitive to various defects in the propagated span. Ultrasonic energy propagating through the steel tube leaks to concrete and water. The leakage into concrete depends on the relative elastic and damping properties of the concrete filled inside. The efficiency of steel-concrete interface bond can be effectively characterized by ultrasonic investigations. The discontinuities and irregularities produced as a result of corrosion and other service related damages in CFST sections would result in scattering and reflections of the smooth wave guide resulting in mode conversions and signal attenuation. Another effect of debonding of steel from surrounding concrete is expected to reduce leakage into the surrounding concrete and signal rise. Therefore, it should be possible to characterize various defects as a result of various kinds of damages in steel tube and interface modifications. It is proposed in this study to utilize specific guided wave modes to monitor various kinds of damages in CFST sections using this non-contact guided wave technique.

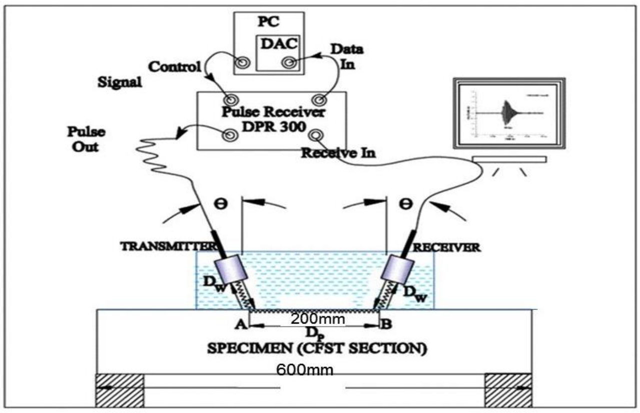

(a) Schematic of Ultrasonic testing set-up

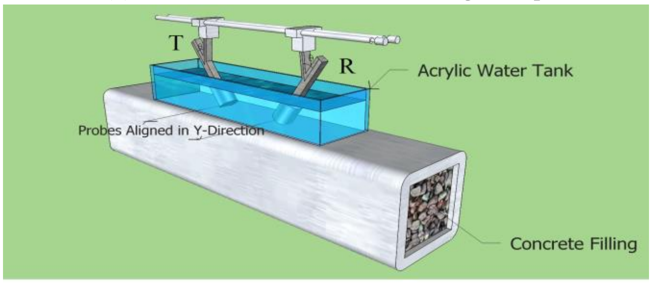

(b) Schematic of probes

Fig. 1 Experimental Set-Up

3. Experimental preparation and methodology

It is proposed to study the effect of area loss and debond of the steel tube from the surrounding concrete in CFST sections using ultrasonic guided waves. The changes in ultrasonic transmitted signal with increasing depth of the notches and with increasing length of delamination would lead to damage diagnosis of the CFST tube. Area loss is simulated as notches of varying depths in steel tube and increasing delamination is simulated as loss of bond between steel tube and concrete using a double-sided tape of increasing lengths.

3.1 CFST sample preparation

The square hollow steel tubes confirming to IS 4923 - 1997 and IS 1161-1998 having a cross-section of 72 mm×72 mm×3.2 mm have been used in the study as these were easily available in the market. Moreover, the change in geometry (thickness) and material properties will not change the methodology overall. The length of the square hollow steel tubes was kept 600 mm. These hollow steel tubes were filled with commonly used M-25 grade concrete with design mix proportions of cement, sand and stone aggregates as 1:1.375 (FA):1.539 (20 mm CA) :1.510 (10 mm CA) by weight prepared with water cement ratio of 0.44. The 28 days' compressive strength of cubes was found to 38.7 N/mm^2.The steel tube was left unfilled by 25 mm on each side of the section for attaching clips to use it as anode and for easy handling of samples. Total twelve samples were prepared to be used for different purposes. The CFST specimens were cured for 14 days and left for drying in air for another 14 days.

3.2 Ultrasonic testing system and set up details

The ultrasonic testing (UT) system consists of DPR300 Pulser/Receiver system (Karl Dutsch Make) (Fig. 1(a)), transducers (Olympus NDTT Immersion Probes), data acquisition system and display devices (Sharma and Mukherjee 2015a, b, Garg *et al*. 2016). The compression transducers are driven by the PR system which generates ultrasonic pulses through the steel tube of CFST section. The ultrasonic excitation is a pulse obtained when PR is set at maximum input voltage amplitude of 475V. The ultrasonic waves generated by the transmitter probe travel through the surrounding water and intrude the tube of CFST specimen at an angle to generate the corresponding Lamb wave mode. The probes are to be placed at an appropriate distance from the plate specimen which is termed as *Water Path*. It is the distance travelled in water before the wave hits the top surface of the CFST section. Transmitter transducer sends the ultrasonic pulse to the specimen through a coupling medium (water) and is received by the receiving transducer. The received pulses are the pulse transmission signals displayed in the form of Voltage- time (V-t) signatures. In this study, non-contact transducers of 0.5 MHz and 1.0 MHz are used. The selection of typical frequencies for UT is discussed in the following section.

3.3 Selection of optimum mode and frequency

Lower frequencies of 0.5 MHz and 1.0 MHz were initially selected for experimental study due to lesser dispersion at lower frequencies. The probes at these frequencies were used for checking the signal fidelity and signatures were obtained at various angles of inclination of T and R probes. In order to avoid any bias in the experiment, P-R settings were kept constant during the study. The propagation span was kept as 200 mm and water path of 30 μs was chosen for both left transmitting and

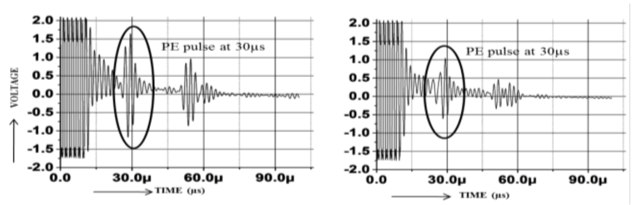

(a) PE signatures at 0.5 MHz frequency
Left probe Right probe

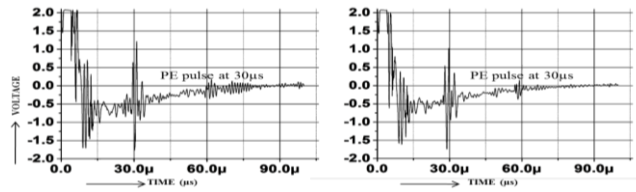

(b) PE signatures at 1.0 MHz frequency
Left probe Right probe

Fig. 2 Typical PE signatures to set the water-path

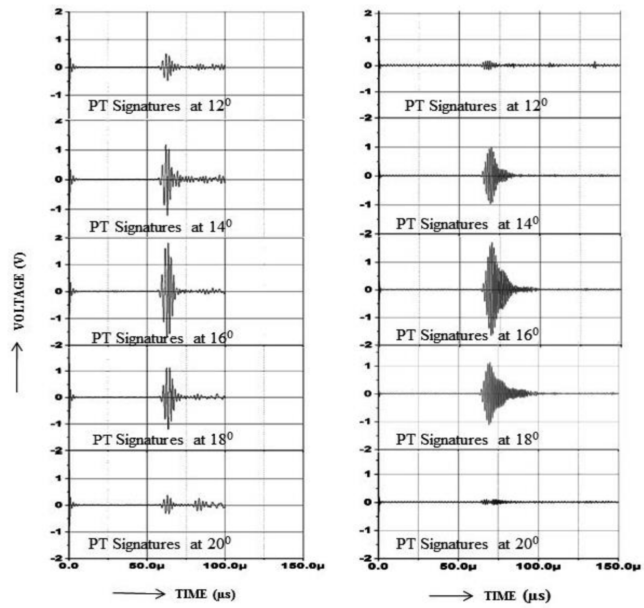

(a) 0.5 MHz (b) 1.0 MHz

Fig. 3 PT signatures at varying angles (a) 0.5 MHz (b) 1.0 MHz

Right Receiver probe (Fig. 2).

Pulse transmitted signals obtained at 0.5 MHz by varying the incidence angles are shown in Fig. 3(a) and the corresponding peak to peak voltage trends of the received PT signals are shown in Fig. 4(a) respectively. It is observed that as the angles of probes is varied from 12° onwards upto 16°, signal strength rises significantly but further starts falling with increase in angle beyond 16°. From the observed signals and their trends, the best signal fidelity and pulse is obtained at 16°. From the phase velocity, angle of incidence with water and attenuation dispersion curves (Fig. 5) plotted using software Disperse (Pavlakovic and Cawley 2000), for 3.2 mm thick steel plate with water on one side and concrete on the other, it is observed that the signal at 16° corresponds to S_o mode at

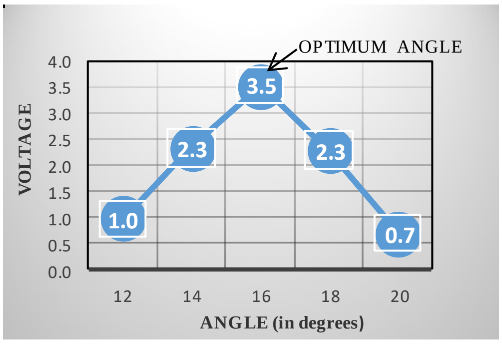

(a) 0.5 MHz

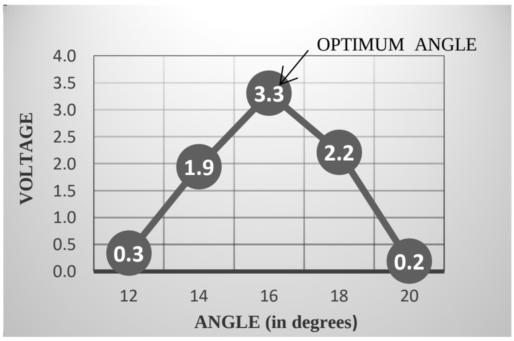

(b) 1.0 MHz

Fig. 4 Peak to Peak voltage trends at varying incident angles

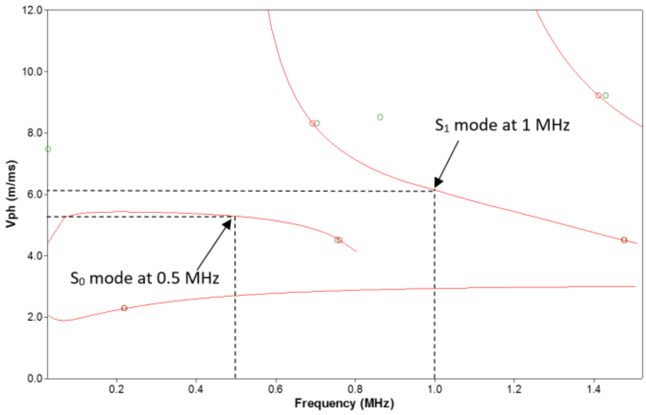

(a) Phase Velocity Vs Frequency

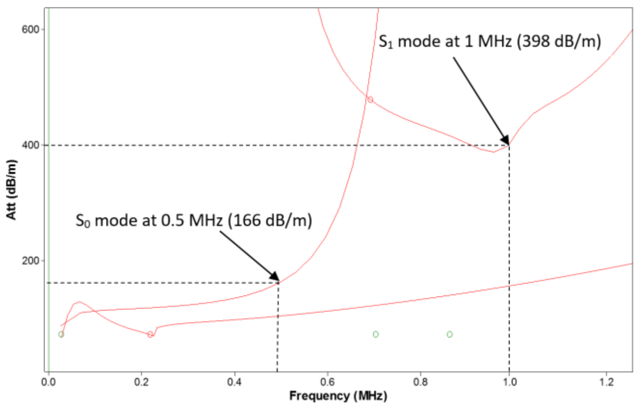

(b) Angle of Incidence with Water Vs Frequency

Fig. 5 Dispersion curves (Pavlakovic and Cawley 2000)

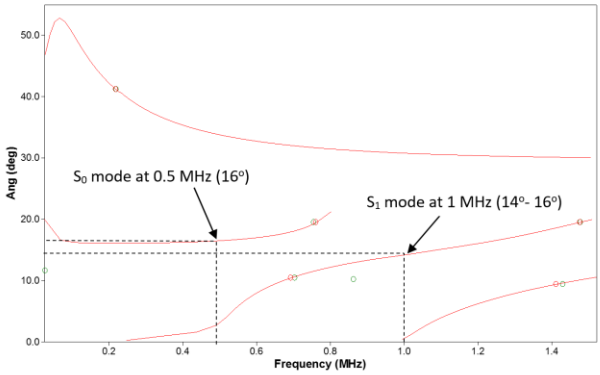

(c) Attenuation Vs Frequency

Fig. 5 Continued

0.5 MHz.

Similarly, PT signatures at 1 MHz (Fig. 3(b)) by varying the incidence angles and corresponding peak to peak voltage trends of the PT signals have been obtained (Fig. 4(b)). Rise in signal strength is observed as the angles of probes is varied from 12° onwards upto16° which starts falling with further increase in angle. The best signal fidelity in healthy CFST tube is also obtained at around 14°-16° from the observed signals and their trends. From the phase velocity and angle of incidence with frequency dispersion curves (Fig. 5(b)), it is observed that the mode at 14°-16° corresponds to S_1 mode at 1 MHz

From the attenuation dispersion curves also (Fig. 5(c)), it is observed that the two modes are least attenuative at these frequencies. Hence, the two modes of S_0 at 0.5 MHz and S_1 at 1.0 MHz are used further for experimental investigations.

4. Damage detection in CFST

4.1 Simulated defects

4.1.1 Notches in tubes

PT signatures in the healthy CFST specimens were taken using the selected S_0 mode at 0.5 MHz and S_1 mode at 1.0 MHz frequencies respectively. Simulated defects in the form of machined notches of varying depths (1 mm, 2 mm, 3 mm and 3.2 mm) were machined in the middle of the steel tube of CFST section as a through cut. A total of four specimens each reflective of a particular notch depth were fabricated. The width of the notches was kept constant of 2 mm.To ensure repeatability of the experiments and the readings, the signatures were taken on three locations marked on the steel tube as Loc-1, Loc-2 and Loc-3 (Fig. 6). PT signatures corresponding to increasing depths of notches were recorded to study the effect of these damages on signal strength. Comparison of PT signatures of simulated notched specimens vis-a-vis healthy specimens was done to quantify the effect of notches on signal strength.

4.1.2 Debond/ Delamination of steel tube from in filled concrete

Another set of three specimens with increasing length of debond between tube and concrete and one specimen without debond (Healthy) was prepared. Debonding between steel and concrete was created by pasting square sized PVC sheets of various sizes 40 mm×40 mm (S1), 50 mm×50 mm (S2) and 70 mm×70 mm (S3) to inner surface of hollow pipe in the middle portion of steel tube prior to filling the concrete inside (Fig. 7). This indicated increasing debond between steel tube and concrete of CFST section. The PT signatures were also taken on these simulated debond samples and compared with healthy signal to study the effect of delamination on PT signals. In this case also, the signals were taken at three locations in a particular sample.

5. Results and discussions

5.1 Simulated notch defects

Using S_0 mode at 0.5 MHz frequency, ultrasonic pulse transmission signatures are recorded at three different locations (Fig. 6) at a gap of 25 mm (each side from centre line of sample) with increasing depths of notches. It was done to ensure whether at all locations fall in voltage amplitude is consistent or not, due to presence of notch to mark repeatability of results. D_p was fixed as 200 mm with water path of 30 µs. PT signatures obtained with S_0 mode at 0.5 MHz with increasing depth of notches in simulated notch specimens are shown in Fig. 8(a). The trends of the transmitted signals with respect to healthy voltage amplitudes are plotted in Fig. 9(a).

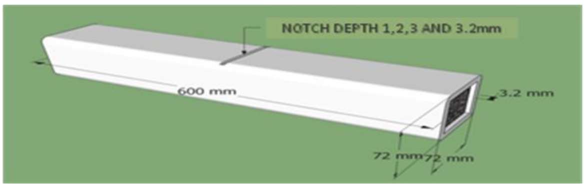

(a) Schematic

(b) Actual specimen

Fig. 6 Simulated notch specimen (Notch in middle)

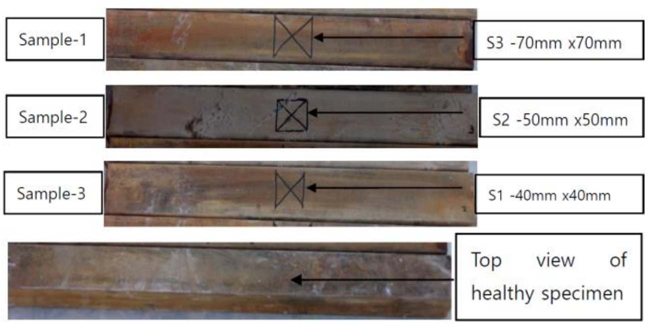

Fig. 7 Simulated debond specimens

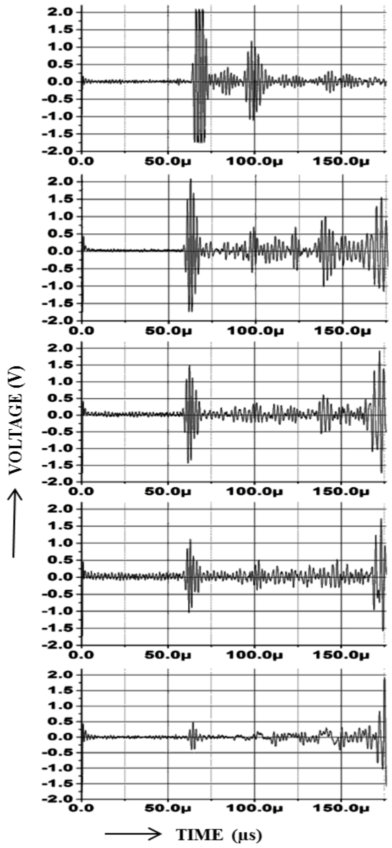

(a) S_0 mode at 0.5 MHz frequency

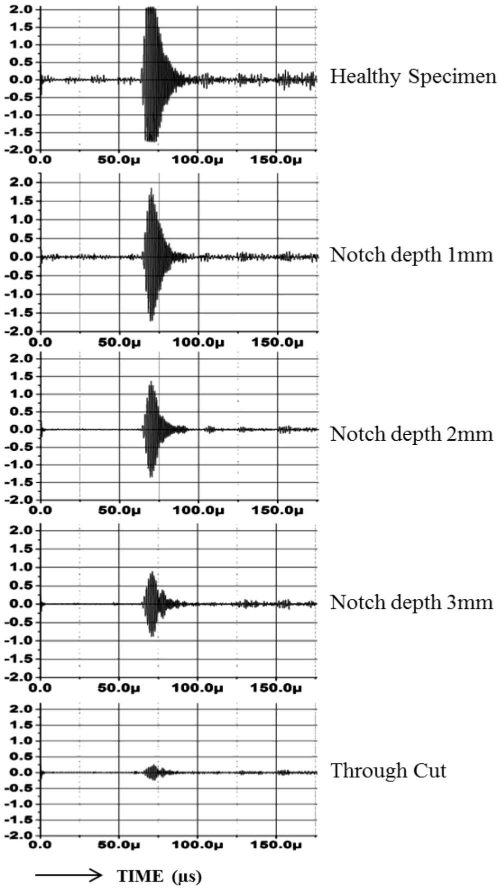

(b) S_1 mode at 1.0 MHz frequency

Fig. 8 PT signatures in simulated notched specimens

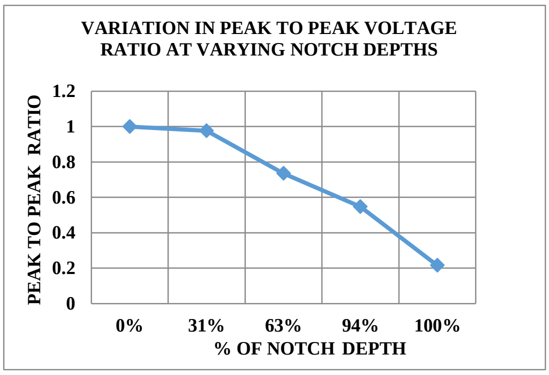

(a) S_0 mode at 0.5 MHz frequency

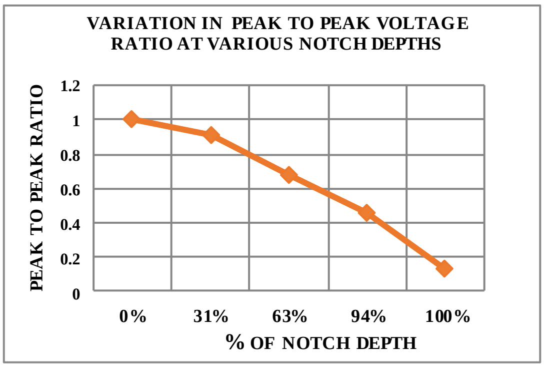

(b) S_0 mode at 1.0 MHz frequency

Fig. 9 Normalized peak to peak voltages for simulated notched specimens

From the transmitted signal strength (Fig. 9(a)) in notched specimens, it is observed that there is drop in signal strength as the depth of the notch increases. This is due to increase in reflections from notch with increased depth and less energy being from notch with increased depth. The drop in the voltage amplitude of the received signal indicates the presence of notch as compared to healthy signal. Also with increase in depths of notch, signal strength constantly drops and here the comparison of healthy signals with signals obtained in notched specimen can be used to quantify the extent of notch also.

Similarly, pulse transmission signals are recorded on the same specimens using S_1 mode at 1.0 MHz as shown in Fig. 8(b). It is observed from pulse transmission signals that as the depth of notch increases there is constant drop in signal amplitudes. At through cut, the signal received is of almost negligible magnitude.

From the PT signatures obtained using S_0 mode at 0.5 MHz and S_1 mode at 1.0 MHz it is observed that the amplitude of the peak to peak voltage of the received signal decreases with increase in the depth of the notch. S_0 mode at 0.5 MHz shows a clear and significant peak and consistent drop in voltage amplitudes with increasing depth of notch defects. It is due to lesser signals attenuation and scattering at low frequencies. Hence, PT signals at S_0 mode at 0.5 MHz and S_1 mode at 1.0 MHz can be used to identify as well as quantify the notch defects and would be further used for identifying actual corrosion in CFST sections.

5.2 Simulated debonds defects

Ultrasonic pulse transmission signatures were recorded in healthy CFST specimens and compared with the signatures obtained with increased debonding using both S_0 mode at 0.5 MHz and S_1 mode at 1.0 MHz respectively. PT signatures recorded using S_0 mode at 0.5 MHz with increasing debond are shown in Fig. 10. Voltage amplitudes of the received signals with increased delamination with respect to healthy signals are plotted in Fig. 11. It is observed that there is increase in the ultrasonic signal as the area of delamination increases. As the debond increases, there is a rise of 38.4% in S1, 56.8% in S2 and 94.3% in S3 as compared to healthy signal. This is due to reduction in leakage of signal with increase in delamination causing rise in signal strength. Hence, increase in signal strength points towards delamination of the tube from surrounding concrete. Quantitative change in signal amplitude can be used to correlate with the extent of delamination. Similarly, PT signatures for S_1 at 1.0 MHz frequency by increasing area of delamination are shown in Fig. 12 and 13 respectively. The corresponding rise in signal amplitude is observed as 41.8% in S1, 52.6% in S2 and 81.7% in S3 as compared to healthy signal. Hence, increase in debond is marked by rise in signal strength is well picked up by the low frequency mode. The investigation using the two low frequency modes are further used for picking up actual corrosion in CFST sections.

6. Accelerated corrosion studies

This study is further extended to monitor actual accelerated corrosion in CFST sections. The progression of ultrasonic guided waves in steel tubes undergoing corrosion in chloride environments is studied. Two guided wave

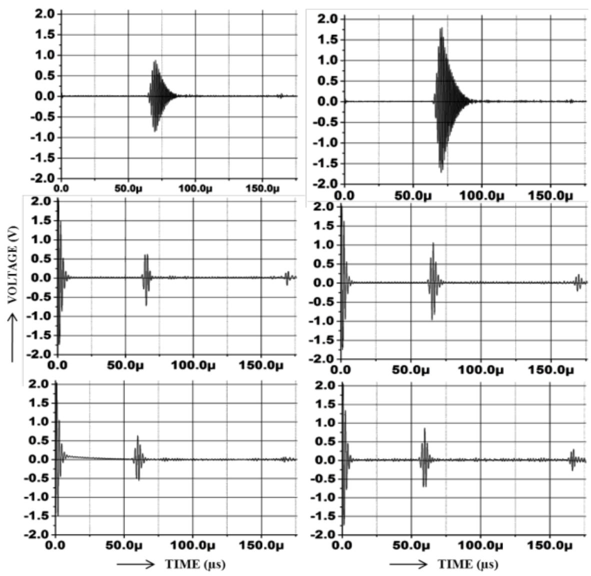

(a) Healthy specimens (b) Specimens with delamination

Fig. 10 PT signatures with increasing delamination (S_0 mode at 0.5 MHz frequency)

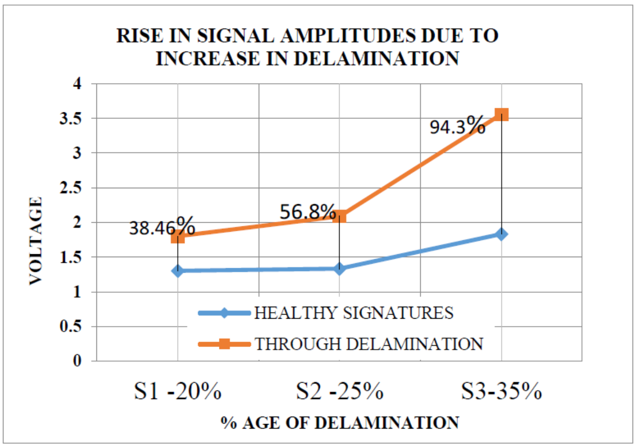

Fig. 11 Comparison of Peak to peak voltages of PT signals of delaminated specimens with healthy specimens with (S_0 mode at 0.5 MHz frequency)

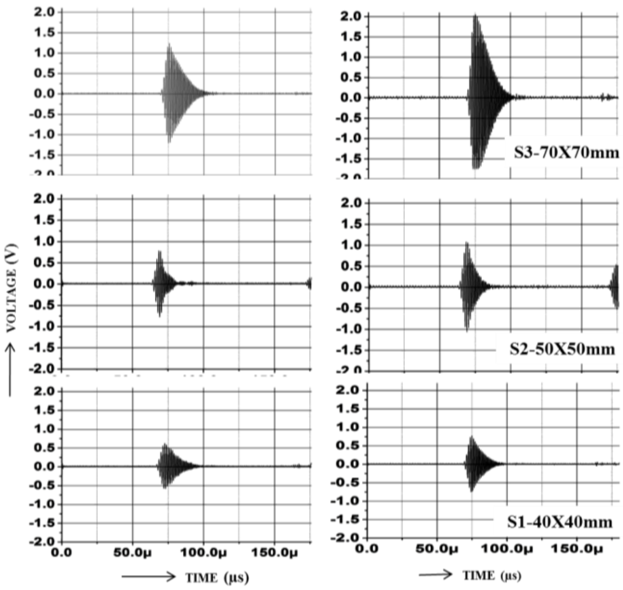

(a) Healthy specimens (b) Specimens with delamination

Fig. 12 PT signatures with increasing delamination (S_1 mode at 1.0 MHz frequency)

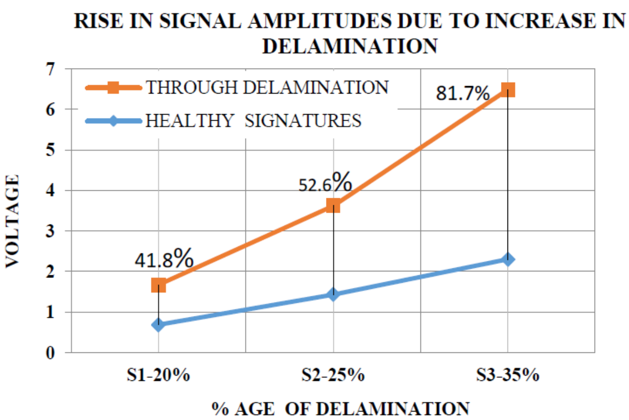

Fig. 13 Comparison of Peak to peak voltages of PT signals of delaminated specimens with healthy specimens (S_1 mode at 1.0 MHz frequency)

modes used in notch and debond studies were further used to evaluate their suitability in discerning different stages of corrosion in CFST sections. A brief discussion on the corrosion mechanism of steel is necessary to understand the proposed method.

6.1 Corrosion in CFST sections and ultrasonic investigations

Corrosion is a destructive phenomenon and in some cases, causes material failure. Corrosion is the process of metal wastage produced by chemical action (oxidation). Natural corrosion takes long time, hence accelerated corrosion has been used to corrode the CFST sections. Commonly used methods of accelerated corrosion are:

- Electrolysis corrosion/Impressed current corrosion method
- Dipping in acidic solution
- Salt mist chamber
- Alternate drying and wetting

Out of these techniques, impressed current technique has been used because it is the fastest and quickest way of inducing corrosion. In impressed current corrosion technique two dissimilar metals are kept in an electrolyte and also having external electrical contact with each other. At least one of the metals must have a positive oxidation potential. A potential difference due to the different oxidation potentials of the metals causes electrons to flow in the circuit. Oxidation (corrosion) occurs at the anode where metal is removed. Reduction (of electrolyte) occurs at the cathode.

Mild steel hollow square sections of dimensions and sizes as mentioned in Section 3.1 filled with concrete were further exposed to accelerated corrosion environment. Weight of the healthy CFST sample was recorded. Impressed current corrosion was done only for a localized area of 140 mm×50 mm dimension. An acrylic pond of dimension (150 mm×60 mm×50 mm) was fixed at the top of the CFST section for restricted exposure to corrosion. Tank was sealed by epoxy to avoid any leakage of the electrolyte. The tank was filled with water with 3.5% NaCl solution to provide chloride environment and induce faster corrosion which was changed everyday till the total duration of exposure. For accelerated corrosion, positive terminal of a constant power supply device (APLAB Make, 0-64V, 0-2 A) was attached to exposed unfilled part of CFST steel tube section and served as anode. An external cathode of copper strip (125 mm×30 mm×4 mm) was used as cathode. This copper strip acting as cathode was kept immersed in acrylic tank within top of CFST specimen. Copper plate is immersed such that it does not touch the surface of CFST specimen. PT signatures were recorded with S_0 mode at 0.5MHz and S_1 mode at 1.0MHz respectively with increasing days of corrosion exposure and compared with healthy signals.

Ultrasonic pulse transmission signatures were recorded using S_0 mode at 0.5MHz and S_1 mode at 1.0 MHz respectively at different locations of the sections as shown in Fig. 14. A constant voltage of 30V was maintained for accelerated corrosion and was continued for 24 hours. After

24 hours, the current was recorded as 0.21A. The acrylic pond was dismantled and PT signatures were taken at all locations and mass were recorded. The acrylic pond was reconstructed and corrosion continued till it gave way to small pits in the top surface of steel tube of the specimens after 13 days. PT signatures were taken after every day at all the marked locations with increased exposure to corrosion.

The PT signatures using S_0 mode at 0.5 MHz and S_1 mode at 1.0 MHz are shown in Fig. 15. PT trends of received voltage signals are shown in Fig. 16. From the signals, it is observed that in the healthy specimen, the signatures are characterized by a strong pulse. For the initial three days with S_0 mode at 0.5 MHz and initial 6 days with S_1 mode at 1.0 MHz there is no significant drop in signal. As the corrosion progresses further in both modes, drop in voltage of the transmitted signal is observed. It is noted that the maximum drop in voltage amplitude is observed at location L-1marked at 25mm from centre line (refer Fig.14). It suggests significant localized corrosion at this location. This can also be visually verified by development of large sized localized pits at the same location. The drop in the PT signal strength can be recognized as the corrosion in CFST sections in exposed part leading to the material loss in the form of pits on the specimen as in case of notches. Initially this voltage drop is found very sluggish but as the corrosion increases this drop is significant due to initiation of formation of small pits at the exposed area. This continues till peak to peak voltage dropped to a very small value on 13th day when large pits appeared on the top surface. Hence, it is indicated that ultrasonic guided wave modes can successfully pick up deterioration due to corrosion in CFST sections. It is marked by severe signal attenuations with increased exposure to corrosion. It is analogous to the increased notch depth in simulated specimens where the signature drops significantly with the increased depth of notch. Hence, chloride corrosion causes pits in steel section similar to notches which are indicated well by signal attenuation of selected guided wave modes. Hence, the damage in the form of simulated notches and debonds and actual corrosion in CFST sections are well picked up by ultrasonic guided wave modes using this non-contact guided wave monitoring technique.

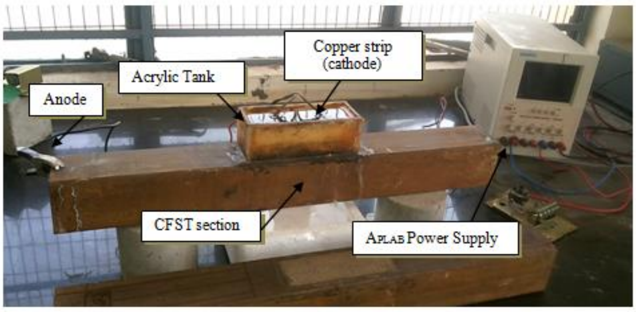

(a) Set- up for accelerated corrosion in CFST sections

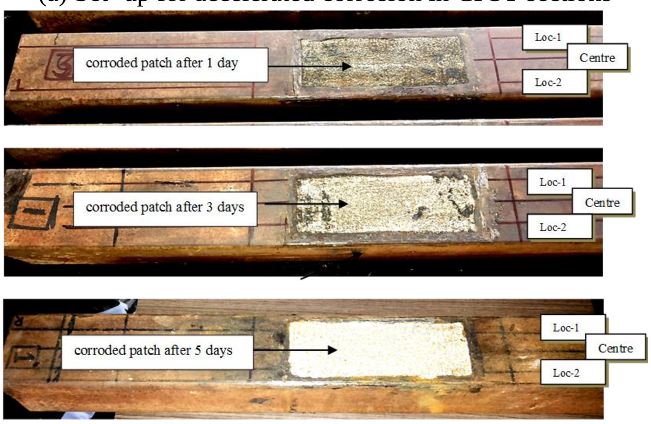

(b) Corroded patch after exposure of increasing days of corrosion

Fig. 14 CFST sections subjected to corrosion

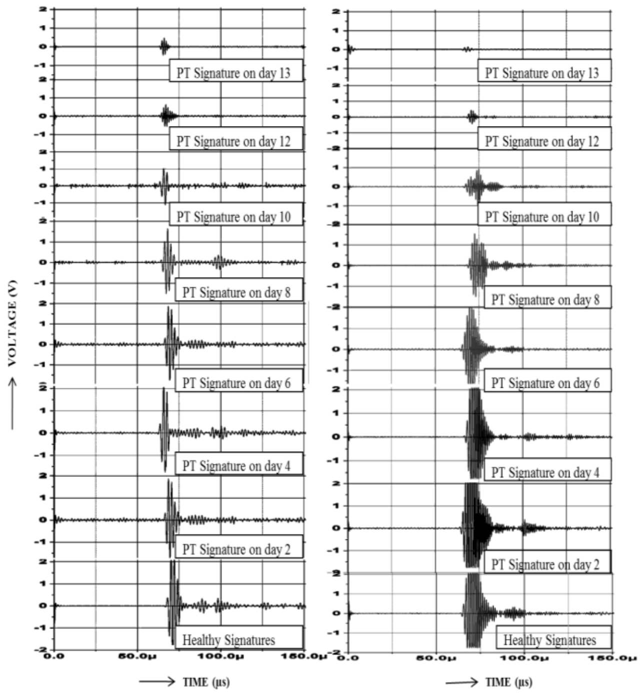

(a) S_0 mode at 0.5 MHz frequency

(b) S_1 mode at 1.0 MHz frequency

Fig. 15 PT signatures with increasing exposure of corrosion

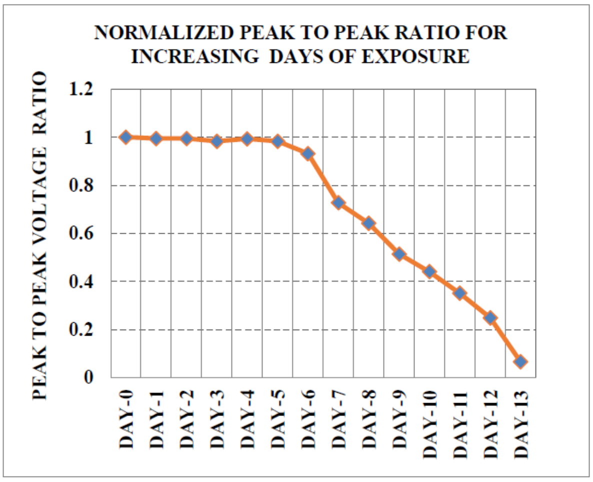

(a) S_0 mode at 0.50 MHz frequency

Fig. 16 Trends of normalized PT signals

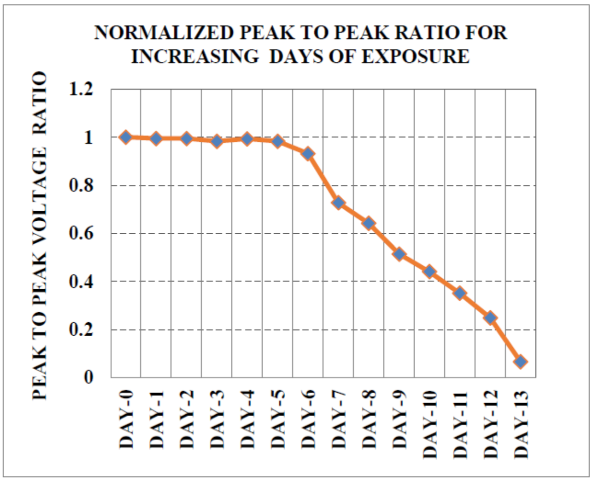

(b) S_1 mode at 1.0 MHz frequency

Fig. 16 Continued

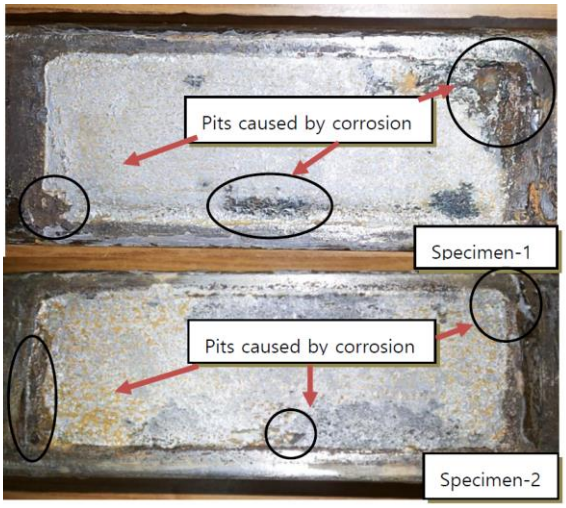

Fig. 17 Formation of pits due to corrosion in CFST specimens

6.2 Destructive testing

Along with the ultrasonic investigations, the samples undergoing corrosion were also monitored for loss in mass with increasing every day. To investigate the effect of corrosion on CFST sections, destructive flexural tests were performed on healthy and two corroded specimens with 6 days and 12 days' corrosion under two-point static loading. Fig. 18 shows the load-deformation curves for healthy and corroded CFST sections. From the P-Δ curves, it has been observed that as the corrosion progressed, flexural strength dropped due to increasing pits and degradation. The flexural strength reduced by 9.82% with 6 days of exposure to accelerated corrosion in comparison to the healthy specimen. After 12 days of exposure, the flexural strength drops by 23.6% in comparison to the healthy beam. Visual inspection also confirmed that as the exposure to corrosion increases, beams experience severe and widespread pitting (Fig. 17). It is also observed that as exposure to corrosive environment increases, % loss in mass of the sample w.r.t mass of healthy sample increases. Initially mass is almost negligible at 7 days of corrosion. This signifies that the initial corrosion is slow and it does not lead to a significant mass loss. At the start of pitting, after the 7th day, there is significant loss of mass and at 12 days 1.15% mass loss is observed. Results of destructive testing of healthy specimen, 6 days corroded specimen and 12 days corroded CFST specimen are presented in Fig. 19 and Table 1.

P-Δ results indicate the ductile behaviour of CFST sections. As corrosion increases, the ductility is reduced. It is observed that at peak load 61.42 KN, displacement is 7 mm in healthy CFST sections, which increases to 15 mm at load of 64.77 KN and still no crack was observed on the specimen. In partially corroded samples the peak load and displacement is 58.41 KN and 10.25 mm respectively and in fully corroded samples with increased corrosion, the strength falls to 49.46 kN and brittleness increases which can be very catastrophic if not monitored properly and at early stages. It indicates the importance of monitoring of progressive corrosion and other defects in CFST sections much before the sections completely collapse.

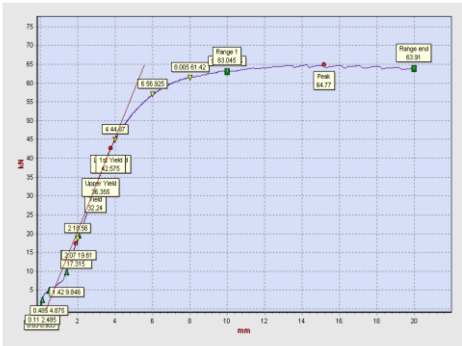

(a)

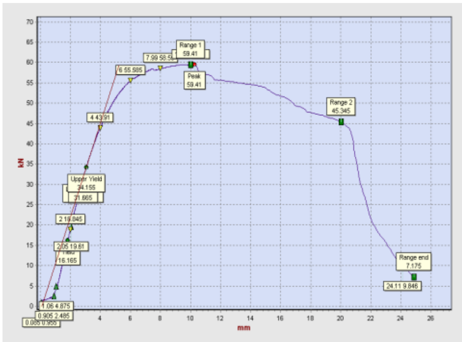

(b)

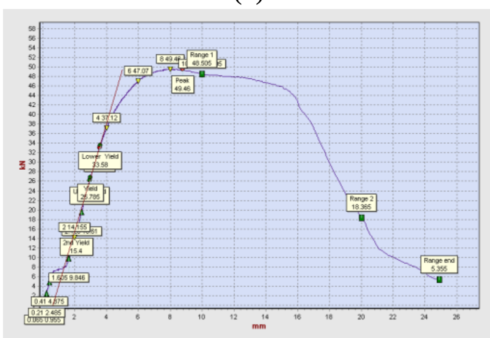

(c)

Fig. 18 Load v/s Displacement curves of (a) Healthy, (b) 6 days corroded and (c) 12 days corroded CFST specimens

Table 1 Results for Flexural testing of corroded CFST specimens

Sr. No.	**Results for testing of CFST specimens**			
1.	Days of Corrosion Exposure	0 (Healthy)	6	12
2.	Mass Loss (%)	0	0.547	1.15
3.	Peak Strength (kN)	64.77	58.41	49.46
4.	Displacement (mm)	15.0	10.25	8.49

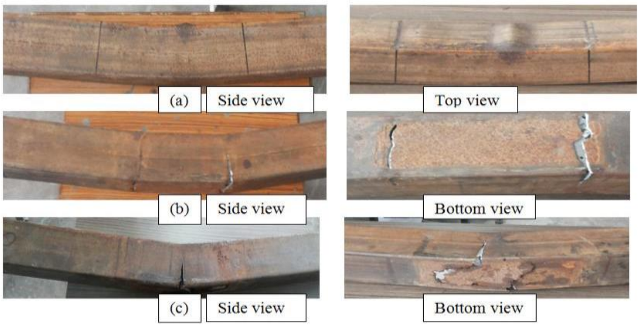

Fig. 19 Flexural Testing of (a) Healthy (b) 6 days corroded (c) 12 days Corroded CFST specimens

7. Conclusions

The present investigation illustrates a non-contact ultrasonic guided wave approach for detecting and quantifying various kinds of defects in concrete filled steel tubular sections, using a pair of mobile non-contact probes. Pulse transmission scanning of the CFST specimens helps in identifying the problem areas in the steel tube of CFST section due to various kinds of damage in the form of cracks, notches and corrosion. The reduction of the received signal with increased depth of notch could relate to the extent of notch. Further the increase in the received signal strength with increased area of delamination points towards increased debond of steel tube from concrete causing less leakage and rise in signal strength. The methodology is further successfully applied to the CFST specimens undergoing with progressive accelerated corrosion. The attenuation of the received signal strength with increased corrosion points towards the significant area loss and pitting due to chloride corrosion and is well picked up this in-situ and non-contact damage monitoring methodology. The technique developed in the study clearly suggests that non-contact ultrasonic guided wave approach can be used for degradation monitoring in CFST sections Practical application of the methodology would require further investigations of this non-contact procedure without using water as a couplant (Dry testing) and the research is underway and would be published further.

References

Achenbach, J.D. (1984), *Wave propagation in elastic solids*, New York: North-Holland Publishing Company.

Elchalakani, M., Zhao, X.L. and Grzebieta, R. (2001), "Concrete-filled circular steel tubes subjected to pure bending", *J. Constr. Steel Res.*, **57**(11), 1141-1168.

Ervin, B.L. and Reis, H. (2008), "Longitudinal guided waves for monitoring corrosion in reinforced mortar", *Measurement Sci. Technol.*, **19**(1), 1-19.

Ervin, B.L., Kuchma, D.A., Bernhard, J.T. and Reis, H. (2009), "Monitoring corrosion of rebar embedded in mortar using high frequency guided ultrasonic waves", *J. Eng. Mech.*, **135**(1), 9-19.

Garg, M., Sharma, S., Sharma, S. and Mehta, R. (2016), "Non-contact damage monitoring technique for FRP laminates using guided waves", *Smart Struct. Syst.*, **17**(5), 795-817.

Gourley, B., Tort, C., Hajjar, J.F. and Schiller, P. (2001), *A Synopsis of Studies of the Monotonic and Cyclic Behavior of Concrete-Filled Steel Tube Beam-Columns. Structural Engineering Report* No ST-0-4, Dept of Civil Engineering Institute, Technology University of Minneapolis MN, USA.

Hajjar, J. (2000), "Concrete-filled steel tube columns under earthquake loads". *J. Prog. Struct. Eng. Mater.*, **2**(1), 1-10.

He, C., Van Velsor, J.K., Lee, C.M. and Rose, J.L. (2006), "Health monitoring of rock bolts using ultrasonic guided waves", *quantitative nondestructive evaluation, Thompson, D.O. and Chimenti, D.E.(eds), AIP Conference Proceedings*, Aarhus, Denmark, 25-29 June.

Kuranovas, A. and Kvedaras, A.K. (2007), "Behaviour of hollow concrete-filled steel tubular composite elements", *J. Civ. Eng. Manage. 2007*, **13**(2), 131-141.

Li, D., Du, F., Chen, Z. and Wang, Y. (2016), "Identification of failure mechanisms for CFRP-confined circular concrete-filled steel tubular columns through acoustic emission signals", *Smart Struct. Syst.*, **18**(3), 525-540.

Na, W., Kundu, T. and Ehsani, M.R. (2002), "Ultrasonic guided waves for steel bar concrete interface testing", *Mater. Evaluat.*, **60**, 437-444.

Na, W., Kundu, T. and Ehsani, M.R. (2003), "Lamb waves for detecting delamination between steel bars and concrete", *Comput.-Aid. Civ. Infrastruct. Eng.*, **18**(1), 58-63.

Na, W.B., Kundu, T. and Ryu, Y.S. (2002), "Underwater inspection of concrete-filled steel pipes using guided waves", *KSCE J. Civ. Eng.*, **6**(1), 25-31.

Pavlakovic, B.N. and Cawley, P. (2000), *DISPERSE User's Manual* Version 2.0.1.1. Imperial College, 715 University of London, London.

Redwood, M. (1960), *Mechanical Waveguides*, Bristol: Pergamon Press.

Reis, H., Ervin, B.L., Kuchma, D.A. and Bernhar, J.T. (2005), "Estimation of corrosion damage in steel reinforced mortar using guided waves", *J. Press. Vess. Technol.*, **127**(3), 255-261.

Rose, J.L. (2003), "Back to basics - Dispersion curves in guided wave testing", *Mater. Evaluat.*, **61**(1), 20-22.

Rose, J.L., Avioli, M.J., Mudge, P. and Sanderson, R. (2004), "Guided wave inspection potential of defects in rails", *NDT & E Int.*, **37**(2), 153-161.

Sharma, S. and Mukherjee, A. (2010), "Longitudinal guided waves for monitoring chloride corrosion in reinforcing bars in concrete", *Struct. Hlth. Monit.*, **9**(6), 555-567.

Sharma, S. and Mukherjee, A. (2010). "Monitoring corrosion in oxide and chloride environments", *J. Mater. Civ. Eng.*, **23**(2), 207-211.

Sharma, S. and Mukherjee, A. (2013), "Non-destructive evaluation of corrosion in varying environments using guided waves", *Res. Non-Destruct. Evaluat.*, **24**(2), 1-26.

Sharma, S. and Mukherjee, A. (2015a), "A non-contact technique for damage monitoring in submerged plates using guided waves", *J. Test. Evaluat.-ASTM*, **39**(5), 1009-1034.

Sharma, S. and Mukherjee, A. (2015b), "Ultrasonic guided waves for monitoring corrosion in submerged plates", *Struct. Control Hlth. Monit.*, **22**(1), 19-35.

Webb, J. and Beyton, J.J. (1990), "Composite concrete filled steel tube columns", *Proceedings of Structural Engineering Conference*, Adelaide: The Institution of Engineers Australia, 181-185.

Xu, B., Zhang, T., Song, G. and Gu, H. (2013), "Active interface debonding detection of a concrete-filled steel tube with piezoelectric technologies using wavelet", *Mech. Syst. Sign. Pr.*, **36**(1), 7-17.

Xue, J.Q., Briseghella, B. and Chen, B.C. (2012), "Effects of debonding on circular CFST stub columns", *J. Constr. Steel Res*, **69**(1), 64-76.

Yang, M.G., Cai, C.S. and Chen, Y. (2015), "Creep performance of concrete-filled steel tubular (CFST) columns and applications to a CFST arch bridge", *Steel Compos. Struct.*, **19**(1), 111-129.

CC